Continuous Water Clarity Monitoring in Te Waikoropupū Springs

Prepared for Tasman District Council
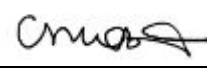
April 2018

Prepared by:
Mark Gall

For any information regarding this report please contact:

Mark Gall
Scientist (Marine Ecology)
Biogeochemistry
+64-4-386 0514
m.gall@niwa.co.nz

National Institute of Water & Atmospheric Research Ltd
Private Bag 14901
Kilbirnie
Wellington 6241

Phone +64 4 386 0300

Revision	Description	Date
Original 1.0	Report prepared for Tasman District Council	13 April 2018
Version 2	Amended to correct Table 3-1, Figure 3-8 and associated text.	11 May 2018
Quality Assurance Statement		
Juliet Milne	Reviewed by:	
Rob Davies-Colley		
Carolyn O'Brien	Formatting checked by:	
Scott Larned	Approved for release by:	

Cover photo: A below surface view of Te Waikoropupū Springs. [Mark Gall, NIWA]

Contents

Executive summary

Tasman District Council (TDC) received a MBIE Envirolink medium advice grant for the National Institute of Water and Atmospheric Research (NIWA) to develop and demonstrate methods to monitor visual clarity at Te Waikoropupū Springs in Golden Bay, including temporal changes in clarity. This involved the evaluation of the results of a short-term deployment of continuous water quality monitoring instrumentation in the main spring. TDC also requested the evaluation of monthly coloured dissolved organic matter (CDOM) measurements as a potential proxy for tracking visual clarity.

For a 3-month period from 13 October 2017 to 18 January 2018, a WET Labs C-Star green beam transmissometer was deployed (suspended) in the main spring to monitor *in-situ* beam attenuation as a basis for estimating visual clarity. A YSI EXO-2 sonde was co-deployed with the transmissometer to continuously measure other water quality properties, including temperature, dissolved oxygen, electrical conductivity, pH, turbidity, and fluorescence of dissolved organic matter (fDOM). Instrumentation was concealed from public view below the water surface, and the base station was set up screened by vegetation on adjacent private land. Monthly servicing, calibration and water sampling were carried out with the assistance of TDC staff, with water samples provided to NIWA Wellington for laboratory determination of light absorption by CDOM on filtrates, using a special 1 m path absorption meter.

Monitoring visual clarity in water of the extreme optical purity of Waikoropupū amounts to pushing the 25-cm path transmissometer well beyond its normal operating range. Ideally a longer path (e.g., 1 m) instrument would be used, but such an instrument is not commercially available. To characterise the extreme visual clarity with existing instrumentation, great care was taken for blanking (minimum transmission) and air (maximum transmission) calibration, and high-frequency sampling was adopted to generate a large amount of data for statistical analysis. One-minute burst sampling (60 readings) at 10-minute intervals, captured nearly a million water clarity estimates, permitting assessment of different time scales of variability from minutes to months.

The visibility over the three-month period, estimated with 'reasonable' (but inevitably uncertain) assumptions about air calibrations and the spectral trend of light attenuation, corresponded to a median of about 77 m (mean 76 ± 7 m standard deviation). About 95% of the time visibility was above 73 m, confirming the extremely high clarity of Waikoropupū. On occasion the inferred visibility (maximum about 81 m) approached that of pure water (about 83 m). Therefore, the clarity regime of Waikoropupū is broadly comparable to that of Blue Lake (Nelson Lakes National Park) in the same region. Furthermore, there is no evidence to indicate that there has been any significant decline in visual clarity in Waikoropupū in the 25 years since the direct measurement of 63 m made by Davies-Colley and Smith (1993).

A small diurnal (daily) cycle of clarity (± 1 m), with highest visibility at midnight, and lowest around midday, is plausibly related to the diurnal cycle of photosynthesis in the springs basin of plants that release (light-scattering) oxygen bubbles during the day. Some short-term (hours to days) episodes of lower clarity coincide with increasing groundwater flow causing accelerating currents which entrain white marble sands and, possibly, finer (more strongly light-attenuating) particulates. Several short-lived (about 12-hour) episodes of rainfall and surface flooding were captured during the deployment with a notable one occurring in mid-January when turbid water entered the main springs basin and resulted in the lowest observed clarity (4 m). Similar reductions in water clarity were observed at Blue Lake, but these were longer-lived, as Blue Lake is a larger system with greater (weekly scale)

residence/flushing times. Overall, the fluctuations observed in visual clarity over the deployment can be attributed to natural variation in rainfall and flow.

Measurements of CDOM served to emphasise the extreme optical purity of water from Waikoropupū. The mean CDOM absorbance at 440 nm was 0.0015 m^{-1}, one of lowest ever reported, and consistent with the blue-violet colour of pure water. CDOM did not contribute detectably to reduced visual clarity in the spring water, and cannot, therefore, be used as an index of visual clarity. However, CDOM is useful in monitoring an aspect of the optical purity of water, its colour (pure water is a blue-violet colour).

This study has confirmed that a WET Labs C-Star 0.25 m pathlength green beam transmissometer (or equivalent) is capable of monitoring temporal changes in clarity in the main spring of Te Waikoropupū Springs by high-frequency monitoring with great care taken with air calibration and blanking. Further, coupling a transmissometer deployment with continuous monitoring of key related water quality variables (temperature, dissolved oxygen and specific conductivity) can help explain observed short-term temporal dynamics in visual clarity and episodic low-water-clarity events.

It is recommended that TDC implement an optical water quality monitoring programme at Te Waikoropupū, including visual clarity and CDOM. Ongoing continuous monitoring may not be necessary. Given the lack of evidence of any significant decline in visual clarity over the last 25 years, an annual or multi-year (e.g., 5-yearly) campaign-based assessment of visual clarity could be considered.   Another approach could be to collect beam transmissometer measurements alongside existing 'seasonal' (3-month) State of the Environment groundwater quality sampling, or monthly surface water quality sampling. Any such *in-situ* discrete (dip-mode) measurements should be made at the same time of day for a stable period, on spring waters not disturbed or contaminated with particulate fines. The timing and duration of monitoring will need to consider the types of small scale and seasonal variability in visual clarity as illustrated in this report (i.e., historical groundwater flow and rainfall data). In addition, the extreme optically-pure water conditions mean that it is essential to strictly adhere to calibration protocols and tracking on each sampling occasion, as outlined in this report.

1   Introduction

Te Waikoropupū Springs are iconic nationally and internationally, for their discharge volume, visual clarity and the blue-violet water colour, which is due to high optical water purity. In 1993, measurements made by the Department of Scientific and Industrial Research (DSIR) determined visibility in the main spring to be 63 m (Davies-Colley and Smith 1995), about 85% of the then expected theoretical maximum (74 m), and the highest reported at that time.

Maintaining the exceptional optical properties of the Springs was identified as a high priority by the Takaka community through a recent collaborative freshwater planning process with Tasman District Council (TDC). This requires estimates of current visual clarity in the springs that are robust and practical to enable the TDC to measure trends in visual clarity through time. Monitoring to date has involved intermittent 'spot' measurements using a beam transmissometer with limited success.

In 2016 NIWA received a MBIE Envirolink small advice grant to evaluate TDC's current field transmissometer methods, provide context in sensitivity and accuracy, and make suggestions and recommendations for future optical water quality monitoring (1721-TSDC127, Gall 2016). This report responds to a subsequent Envirolink medium advice grant (1819-TSDC139) and seeks to demonstrate methods to measure visual clarity in the optically pure Te Waikoropupū Springs, and enable the monitoring of temporal changes in clarity. TDC also requested the evaluation of monthly coloured dissolved organic matter (CDOM) measurements as a potential proxy for tracking visual clarity.

1.1   Background

The only successful direct measurement of visual water clarity in Te Waikoropupū Springs was made 25 years ago using horizontal black disc methods *in-situ* with divers. This required the use of mirrors due to the limited sighting distance (Davies-Colley and Smith 1995). Cultural issues with having divers in the springs has restricted further black disc measurements. Such direct measurements are also impractical on an on-going basis because of the complexity of equipment set-up (mirrors, anchor points), and the 'invasive' and culturally inappropriate character of such measurements in the main springs basin.

Davies-Colley and Smith (1995) suggested that visibility might be higher early in the morning, possibly due to absence of oxygen micro-bubble produced by aquatic plants surrounding the main vent later in the day (pers. comm.). The transmittance measurements taken around midday during field work in 2016 under the earlier small advice grant (Gall 2016) were lower than expected and inconsistent with visual water clarity estimated from coloured dissolved organic matter (CDOM) absorption alone (about 77 m). These 'one-off' measures are not statistically robust (in consideration to accuracy, sensitivity and numbers of observations) to provide a reasonable assessment. Therefore, the effects of diurnal (daily) and temporal variation of visual water clarity warranted further assessment using continuous monitoring.

1.2   Visual water clarity – an overview

Visual water clarity in natural waters is best indexed by the horizontal sighting range of a black body Duntley (1963). Accordingly, the horizontal black disc visibility method was developed by Davies-Colley in the 1980s (Davies-Colley 1988). This visibility metric is strongly (inversely) related to the green beam attenuation coefficient (c), at the wavelength of peak sensitivity of the human eye (550 nm) – Davies-Colley 1988:

$$\textbf{Eq. 1:} \quad y\text{BD} = \frac{4.8}{c_{550}} \text{ (m)}$$

This 'photopic' beam attenuation coefficient (c550) can be estimated from measurements at green wavelengths using commercially available transmissometers (e.g. WET Labs C-Star). When the yBD empirical relationship of Davies-Colley (1988) was reviewed against theoretical models, it was proven to be a robust underwater visibility parameter, accurate with a confidence interval of better than 10% (Zaneveld and Pegau 2003). Instrument monitoring of c550 has advantages over direct measurement of visibility – particularly in that the former can be monitored continuously if required.

The earlier Envirolink small advice grant (Gall 2016) provided context to the sensitivity (and suitability) of two types of green (530 nm) beam transmissometers with varying pathlengths (0.25 m and 1 m), and made recommendations for their use. Although the 1 m pathlength Martek-XMS instrument potentially provides four times greater sensitivity over the 0.25 m pathlength WET Labs C-Star, it is not a practical solution for continuous monitoring for a number of technical reasons including sensor size, current draw from an incandescent lamp light source, and lack of any wiping system to prevent window obscuration. Approaches were made to WET Labs about the possibility of constructing a special 1 m pathlength C-Star for use in exceptionally clear waters, but they declined to do this.

The WET Labs C-Star has a straight 0.25 m pathlength, uses a 'collimated optical system', and is calibrated to pure water, giving a 100% transmittance (Tr) reading (i.e., pure water attenuation subtracted from values). Calibration drift is monitored and adjusted by measuring in air with the light path unobstructed. The path is also blocked to set the zero-transmission point. WET Labs state a precision of about 0.02% and accuracy of beam attenuation of about 0.003 m^{-1}. The quoted accuracy equates to about 0.1% transmission at full scale (100). Expected horizontal visibility distances with a black disk versus expected percentage transmission values are shown in Figure 1-1. These are estimated by conversion of transmittance values to beam attenuation (c) at the wavelength of measurement (c530 nm) by taking the natural log (ln) of the transmittance over the pathlength of 0.25 m, scaling to per meter, and adding the pure water photopic (550 nm) beam attenuation coefficient (cw550 = 0.0579 m^{-1}, see Gall et al. 2013):

$$\textbf{Eq. 2:} \quad c(530) = \frac{1}{0.25}\left(\ln\left(\frac{Tr}{100}\right)\right) + 0.0579 \ (\text{m}^{-1})$$

A shift from an 83 m visibility in pure water to 50 m equates to only a 1% reduction in signal (about 10 times the stated accuracy of the instrument). This highlights that 0.25 m path transmissometers are severely challenged to measure visual clarity in waters with visibility approaching that of pure water. Very careful monitoring of calibration drift is required, and very large numbers of observations are needed for statistical robustness (i.e., the law of large numbers (LLN)).

As the human eye (peak photopic sensitivity of about 550 nm) and the green light of the transmissometer (about 532 nm) are slightly different 'greens', there is a difference in responses due to the type of light-attenuating material in the water. Coloured dissolved organic matter (CDOM – other names are yellow colour, gilvin or gelbstoff), is highly absorbing, with more absorption at shorter (blue) wavelengths. It therefore has more influence on shorter wavelengths (532 nm > absorption at 550 nm). Consequently, if yellow substance dominates attenuation in a water body, the attenuation measured by a 532 nm transmissometer must be adjusted to estimate the attenuation at 550 nm (absorption about 35% less) for the purposes of estimating black disk visibility (Figure 1-1 – orange line). In contrast, suspended particles are likely to have almost the same attenuation (absorption plus scattering) within this green region of the spectrum (532 nm = absorption at 550 nm). If particles dominate attenuation, measurements at 532 nm are expected to

be very similar to those at 550 nm (Figure 1-1 – blue line). These two conditions represent the boundaries in corresponding visibility, whereas the reality may be intermediate (Figure 1-1 – black line).
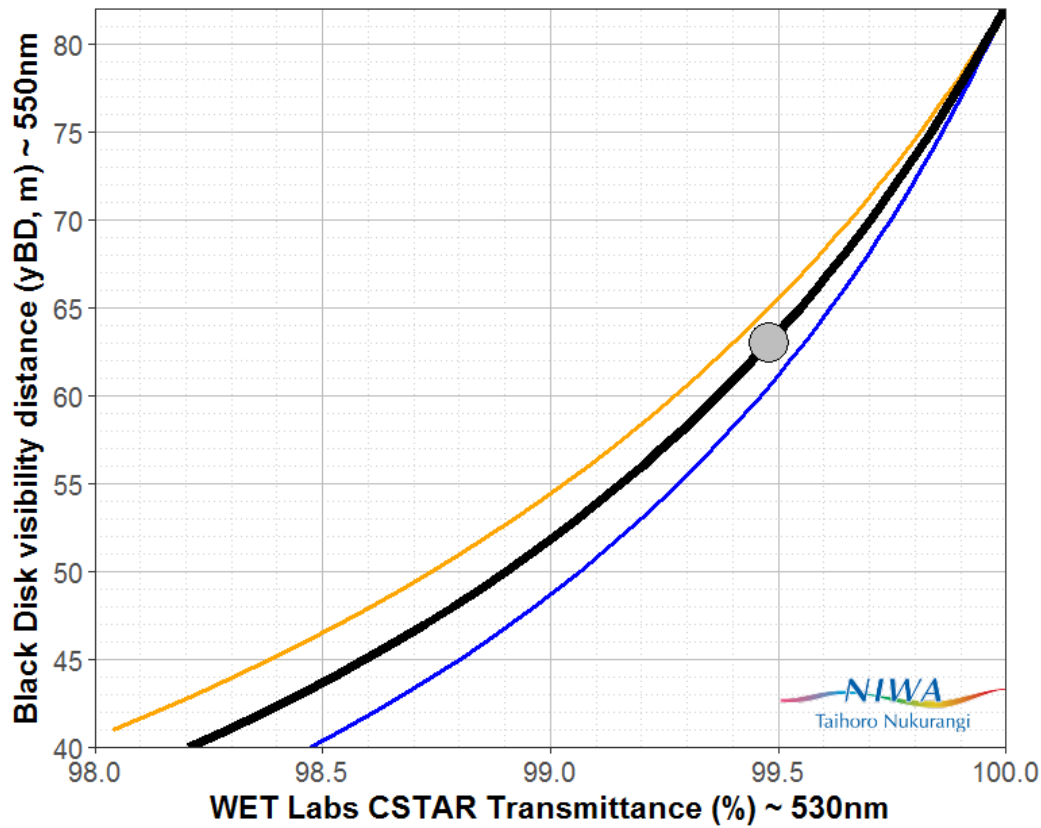
Figure 1-1: Black disk visibility distance against WET Labs C-Star green transmittance values. The C-Star is a 0.25 m pathlength transmissometer. The two outer lines are the effects of different types of material in the water, CDOM (coloured dissolved organic matter – orange) and particles (blue line). The black line is the average of CDOM and particle effects. The grey dot is the estimate for the 63 m visibility reported by Davies-Colley and Smith 1995).

2   Methods

2.1   Site and sampling period

The instrument package for continuous monitoring of water quality was positioned away from the viewing walkway/platform, and close to the deepest basin of the spring (Figure 2-1). Deployment and recovery spanned a 3-month period from 13-October 2017 to 18-January 2018, with monthly servicing in between.
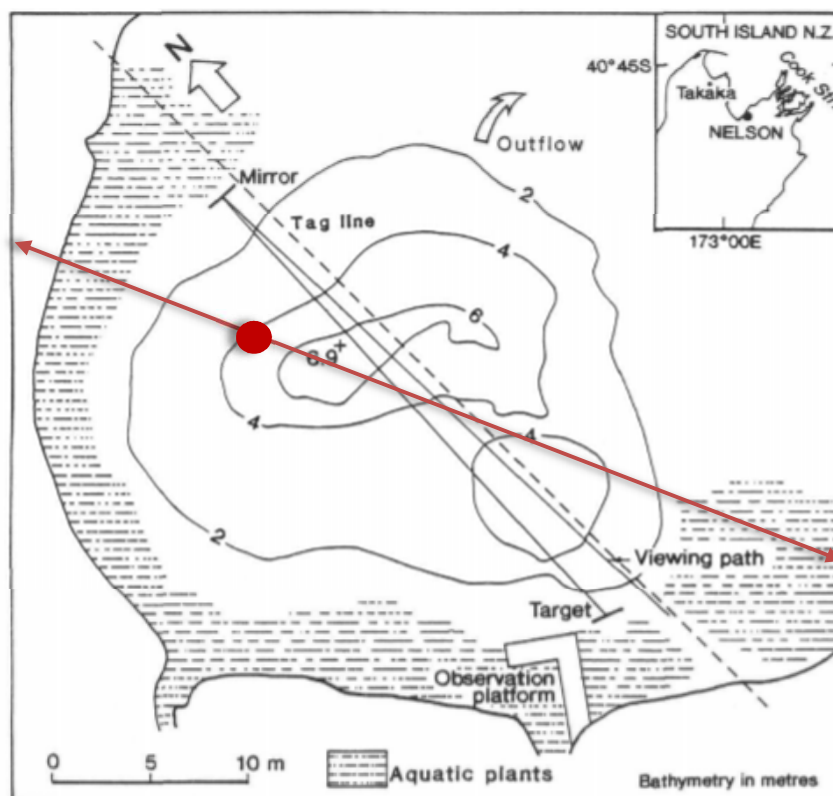
Figure 2-1: Te Waikoropupū Springs bathymetry.   Davies-Colley and Smith (1995) [c.f. Fig. 1, based on data from Michaelis 1976]. The red line and dot (current study) indicates the approximate position of the instrument package and the submersed line used to hang it in position beneath the spring surface. Note: The observation platform has changed to an arched walkway.

2.2   Continuous monitoring equipment

Te Waikoropupū Scientific Monitoring and near-Realtime Telemetry (TE-SMART) was based on a YSI EMM68 telemetry buoy, configured as a land based station to the north-north-east of the spring on private land, with cabling to water quality instrumentation deployed within the main spring. As this is a frequently visited site, with particularly high visitor numbers over the summer period, there was an iwi and Department of Conservation (DOC) requirement to keep the instrumentation well hidden from public view.

A flying fox line was secured across the springs to enable deployment of the instrumentation package from shore (Figure 2-2). Plastic covered mooring wire (5 mm, black) with stainless thimbles secured with wire rope clips, was used for the flying fox cable (about 70 m). A braided fishing haul line was cast across the springs and attached to a buoyed end of the cable to haul across the spring to keep

off the bottom. The cable was anchored to two metal waratah stakes on the opposite shoreline in the bush, out of sight. On the adjacent private land shoreline, a boat trailer ratchet winch on a steel tube was secured into position (backed with waratah stakes), and attached to the flying fox cable. A ladder and hydro bridge-crane was used to raise the cable to height near the shoreline. Tightening the winch, raises the cable out of the springs, providing a sufficient angle for deployment from shore. Once in position, loosening the winch lowers the cable and instrument package to below the spring surface. Removing the ladder/hydro bridge-crane lowers the cable further. The instrument package is recovered using an attached haul line in the opposite manner. Electrical power and communications cables are kept separate from the recovery haul line to avoid tension on connectors.

(A)
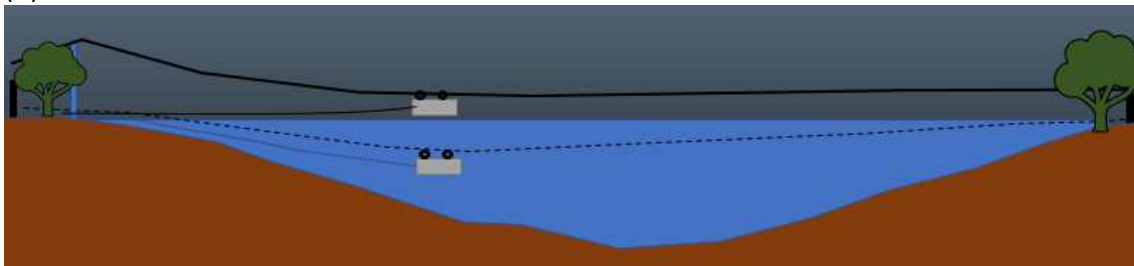
(B)
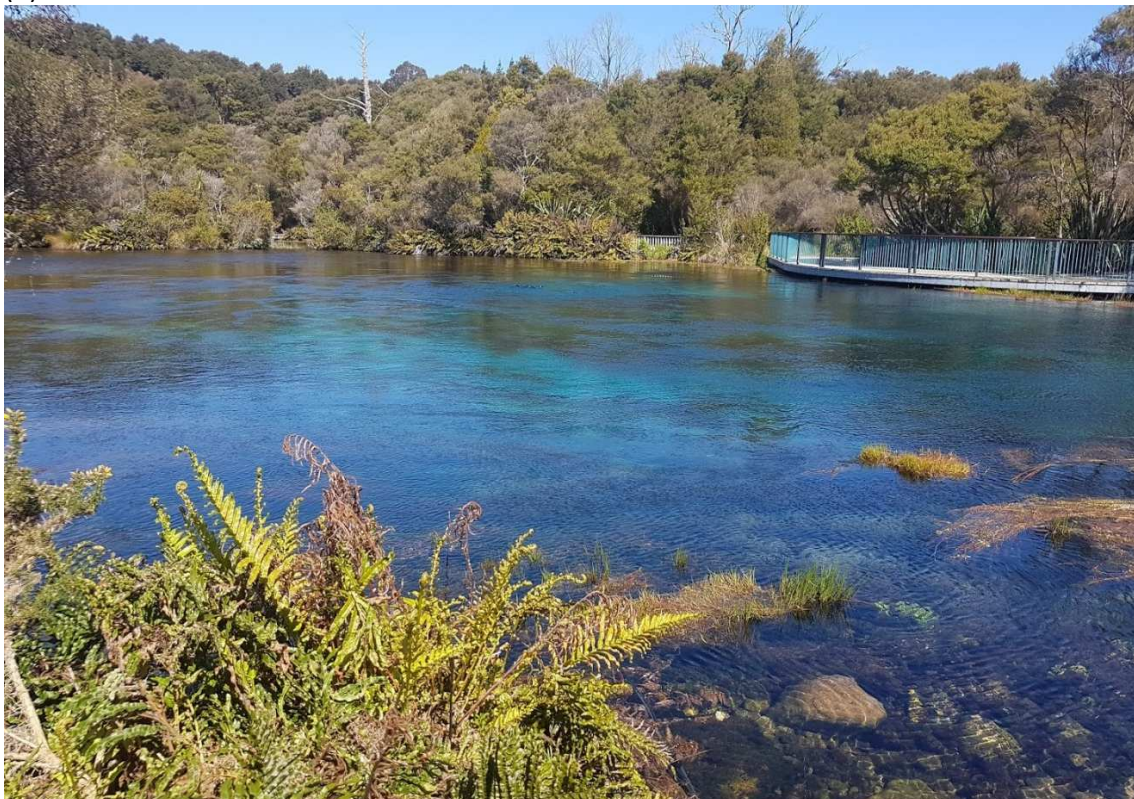
Figure 2-2: Te Waikoropupū Springs instrument flying-fox deployment.   The schematic cross-section (A) viewed from platform looking north, illustrates how the instruments are deployed/recovered from the shore (black line), and when deployed lowered into place (grey dotted line). The package is deployed with a push to send it down to the bottom of the parabolic-shaped flying fox cable, and sits about 20 m from the shoreline. An attached haul line is used for recovery. The photograph (B) is taken from private land on the north-eastern shore, viewing south-east directly above/along the deployment line to the opposite shore, with instruments in position and at depth (out of site).

The main base station was built around a Campbell Scientific CR1000 datalogger, with surface sensors from an AIRMAR 200X weather station and a LiCOR (LI-192) downwelling light sensor (Figure 2-3 A). Power was supplied by two solar panels charging a 24 Ahr battery. Electrical power and communications cables went to the deployed instrument package, which included a XYLEM/YSI EXO-2 sonde (with sensors for temperature, conductivity, dissolved oxygen, pH, turbidity, chlorophyll fluorescence and dissolved organic matter fluorescence), and a WET Labs C-Star 0.25 m pathlength green beam transmissometer (Figure 2-3 B-D). The EOX-2 sonde contains its own wiper brushing unit to keep sensors clean (wipes prior to readings). A ZebraTech Hydrowiper unit specifically designed for a C-Star was fitted to keep optical faces clean (10 min wipe intervals between reading). A burst of 60 readings at 1 hz (1 min collection) was taken at 10 min intervals and telemetered hourly via the Vodafone GPRS network to a NIWA LoggerNet server network. From here the data were exported to the NIWA Neon network for website delivery/graphic near real-time display.

(A)

(B)

(C)

(D)

Figure 2-3: Te Waikoropupū instrumentation.   (A) Base station showing electronic logger housing, frame, solar panels, AIRMAR weather station, light sensor and telemetry aerial. (B) The instrument water quality package showing the C-Star (with ZebraTech wiper unit fitted) strapped to the EXO-2 sonde (above) with the whole package attached to the flying fox cable with pulleys. (C) Flying fox deployment ready to go. (D) Deployed instrument package sitting in position ready to be lowered beneath spring surface.

2.2.1   Sensor calibration

The EXO-2 sonde sensors were calibrated at the NIWA Hamilton water quality laboratory, following guidelines outlined in the EXO-2 user manual. The pH sensor was swapped out on each servicing

period due to known drift issues in very clean waters. Sensor drift was matched to deployment, servicing and recovery field units or laboratory checks. Dissolved oxygen was corrected for drift and aligned with calibrated sonde survey measures bracketing each deployment.

The optical faces of the C-Star were gently cleaned and dried prior to recording at least 1 min of 1 Hz data (60 readings) using the supplied WetView software (WET Labs). Three air readings and one dark reading with the light path blocked were taken on each servicing occasion. Optical faces were recleaned and inspected in between each 1 min reading interval. From these maximum (air) and minimum (blocked) readings bracketing deployments, statistical medians were computed and correction factors (M) and offsets (B) calculated for applying to factory calibrated values following manufacturer protocols and SeaBird Electronics Application Note No. 91 for Wetlabs transmissometers (SBE 2011).

2.2.2   Estimates of horizontal visibility distance

As outlined in Section 1.2, the horizontal visibility distance (yBD – m) was estimated from the simple empirical relationship of Davies-Colley (1988), using estimates of the photopic (eye centered) beam attenuation coefficient (c550 – m^{-1}), by monitoring the green beam attenuation (c532 – m^{-1}) using a 0.25 m pathlength WET Labs C-Star transmissometer.   A c532 ~ c550 (m^{-1}) was assumed in calculations of yBD (blue line in Figure 1-1) – lowest estimates – to allow direct comparison on similar optically pure water in Blue Lake studies (see Gall et al. 2013).

2.3   Discrete water sample collection and CDOM laboratory analysis

TDC staff routinely collect 'seasonal' (3-monthly) spring water samples from the main walkway/viewing platform using an extension sampler pole. Samples are typically analysed at either Hills Laboratories or Geological and Nuclear Sciences (GNS) for a range of water quality variables. Since August 2016, seasonal samples have also been collected for CDOM analysis at NIWA, increasing to monthly intervals during the 2017/18 transmissometer deployment. At the same time as water sample collection, *in-situ* measurements of water temperature, specific conductance, dissolved oxygen and pH are also made by TDC using a YSI ProDSS field meter.

Acid cleaned CDOM bottles (polycarbonate, 50 ml) were rinsed three times with sample water prior to collection in quintuplets, to truly replicate sample collections and laboratory analysis for an accurate measure at that time. Water samples were stored on ice, in the dark, before spectral absorption analysis at NIWA Wellington (typically within 24 hours). In brief, the absorption spectra from 300 to 850 nm was determined through a 1 m long liquid waveguide capillary cell (LWCC - Precision Instruments Inc.), using a UV/VIS light source and spectrometer (Ocean Optics Inc.). Samples were pre-filtered (< 0.45 um cartridge) prior to determination against referenced laboratory nano-pure water. Samples were referenced to a non-pure water blanking, immediately prior to a sample reading. All measurements were carried out at 20 °C.

For comparison to the optically pure Blue Lake, the analysis procedures followed those used by Gall et al. (2013). An exponential fit to CDOM absorption spectra (following Bricaud et al. 1981) was solved for each spectrum between 300 nm and 700 nm, by nonlinear least-squares (nls) regression:

$$\textbf{Eq. 3:} \quad a_g(\lambda) = a_g(\lambda_r) * e^{-S_g(\lambda - \lambda_r)} + b$$

where, ag are absorption coefficients, Sg is the spectral slope parameter, and the term b (baseline) was added to allow the model fit to determine a linear spectral offset. This differs from the spectrally

dependant scattering corrections proposed by Bricaud et al. (1981) - also see Davies-Colley (1992). A baseline accounts for unavoidable shifts between blanks and samplings. This approach is more accurate than selecting a specific long reference wavelength > 700 nm, where temperature dips and noisy spectra are common for these sensitive measures.

2.4   Other data

Groundwater inflow data (m^3/s) were provided by TDC from their ground water level monitoring site (Arthur Marble Aquifer at Te Waikoropupu Springs - GW 6013). Rainfall data (mm/hr) were also provided by TDC from their rainfall monitoring site (HY Takaka at Kotinga). The NIWA Tide Forecaster was used to extract historical records and verify the magnitude of tidal impacts on aquifer flow.

2.5   Data processing and statistical analysis

R statistical software and several packages (libraries) were used for all model fitting, data analysis and graphics (Team 2017). The turbidity sensor data at times were suspect and did not agree with beam attenuation records (either the turbidity sensor was intermittently faulty, or automatic brush cleaning was inadequate). Turbidity values greater than 15-fold that of c532 (about 5% of the data) were removed and replaced with the median of all values (0.035 FTU), to allow a general comparison with other water quality variables, and a verification of changes in water clarity – as turbidity increases, water clarity decreases.

3   Results

3.1   Beam transmissometer calibration

The calibrations in the air (path open – maximum values) and dark (path blocked – minimum values) bracketing deployment periods demonstrate the challenges with obtaining accurate field calibrations for application in optically pure waters such as Te Waikoropupū Springs (Figure 3-1). As there were no differences in replicates of dark readings only single measures were taken (and these are not displayed). Although triplicate air readings did vary significantly, the highest replicate value is likely to be closest to a valid air calibration, as there are challenges in keeping optical faces clean and dust-free during measures in the field.
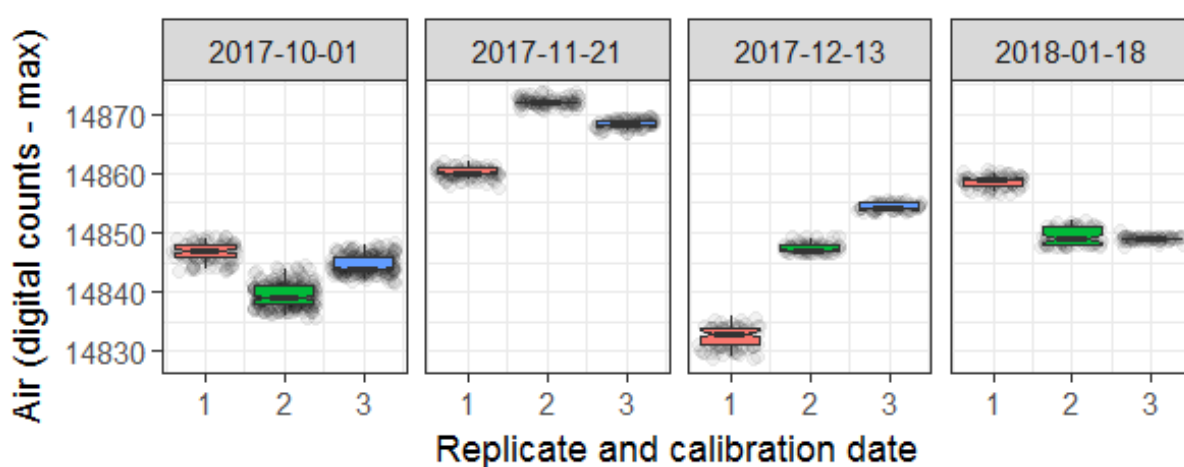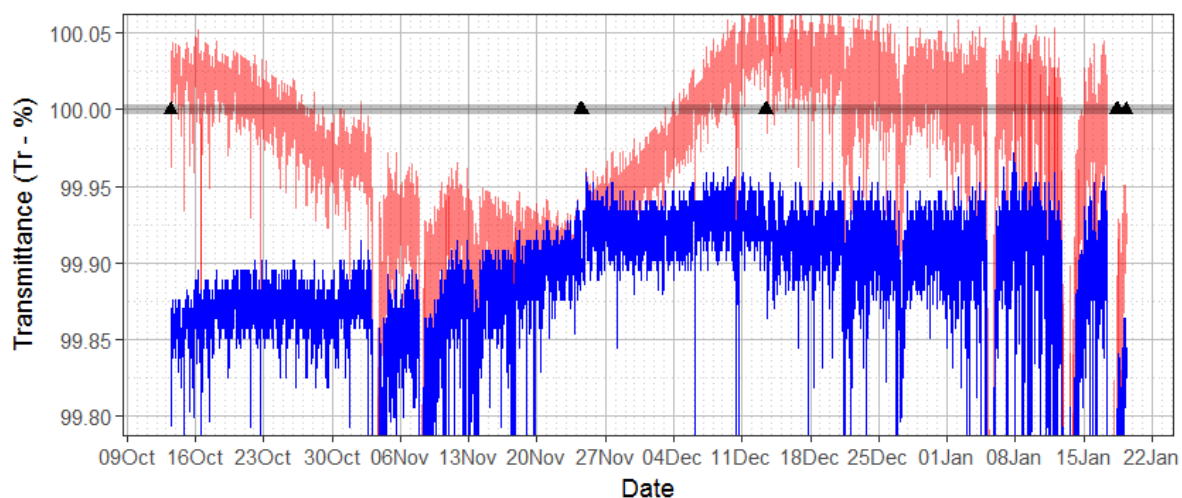

Figure 3-1: Beam transmissometer calibration statistics

   Air (max) replicate measurements bracketing deployments. Boxplots illustrate median values, box interquartile range (IQR – 50% of data), and whiskers 1.5 IQR (99.3% of data). Notches display the 95% confidence interval around the median. A general rule of thumb is when notches are separated, there is likely to be a statistically significant difference between medians (Chambers et al. 1983).

Applying the highest air calibration (which equates to the lowest multiplication factor) bracketing each deployment, with linear adjustments for drift in between servicing (Figure 3-2), produced unrealistic (sometimes > 100%) transmittance time-series (red trace), compared to using the highest air calibration over the entire dataset (blue trace Figure 3-2). The greatest difference in Figure 3-2 is about 0.15 %. If we assume that transmittance values in pure water cannot be > 100% (i.e. beam attenuation < 0 m^{-1}), there is a potential field calibration bias (systematic error) ranging between 99.85 and 100 %. This equates to a beam attenuation range between 0 and 0.006 m^{-1}. The highest median air calibration from all measures was used as the calibration factor in calculations because uncertainty remains in the accuracy of 'real' (laboratory quality controlled) calibration drift over a 3-month period.

Figure 3-2: Beam transmissometer calibration effects on transmittance values. Application of calibrations bracketing each deployment (red) and using the highest air calibration sampling over the entire dataset (blue). Triangles mark the times of deployment, two servicing events, and recovery. Note: Transmittance scaled to highlight calibration effects near pure water conditions (100%).

## 3.2 Beam transmittance, attenuation and estimates of water clarity

Nearly a million C-Star beam transmittance/attenuation values, and corresponding estimates of visual water clarity, were recorded over the deployment period in 60 second bursts at 10-minute intervals. As illustrated in Figure 3-1, relying on field air calibrations bracketing each deployment produced unrealistic transmittance values. The 0.15% percentage transmittance range (0.006 m^{-1} beam attenuation) equates to visual range estimates of between 75 and 83 m (about 8 m in pure water conditions).

Estimates of horizontal visibility distance are also dependent on assumptions made as to the type of light attenuating material in the water (Figure 3-3). As illustrated in Section 1.2 (Figure 1-1), there is likely to be a range to estimates in yBD (m), based on the how the type of light attenuating material (either particles to CDOM) influences estimates of c550 (m^{-1}) from c532 (m^{-1}). If CDOM is dominant c550 will be about 35% less, equating to about a 3 m increase in visibility when visibility is around 75 m, and about a 6 m increase when visibility is around 50 m (Figure 3-3). Particle-based (lower) visibility estimates were used to allow direct comparisons to Blue Lake studies.

The precision and accuracy of estimates are relevant to the analysis of temporal changes and natural variability in water quality. The size of standard error (as well as the standard deviation and confidence interval) within a 60 second burst, was found to vary with the magnitude of the optical attribute, increasing with increasing attenuation or with decreasing transmittance and visibility (Figure 3-4, Table 3-1).
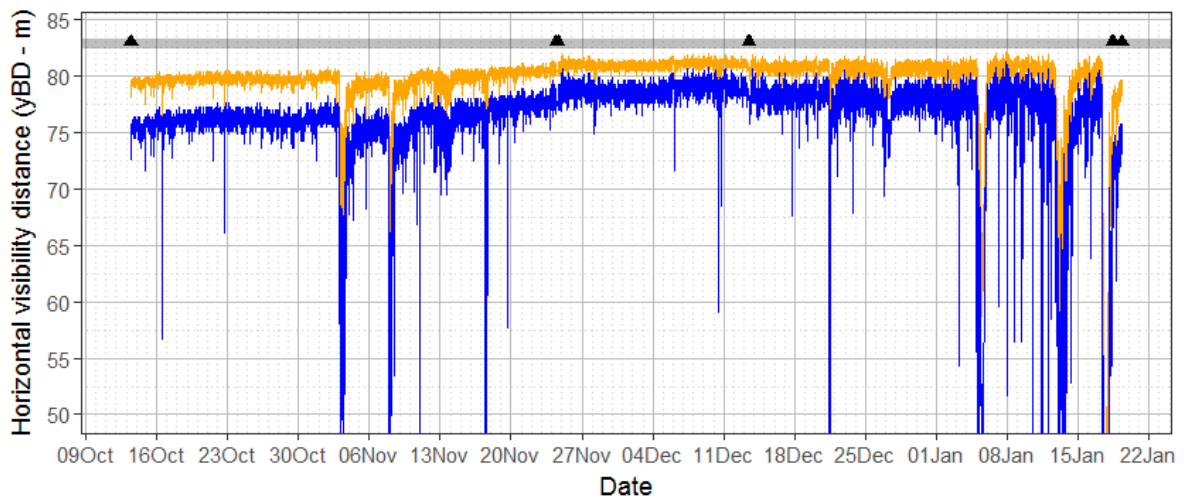
Figure 3-3: Effects of type of light attenuating material on estimates of visibility distance. Particle dominant attenuation (blue line) assumes a flat spectral attenuation shape (c550~c532), as compared to a CDOM dominant attenuation (orange line) assuming an exponentially decreasing shape (c550 < c532 by about 35%). The assumption of a flat spectral attenuation (blue line) seems more likely and was adopted here. Note: Theoretical horizontal visibility maxima (horizontal grey line) is based on a pure water light attenuation of 0.0579 m^{-1}. Triangles illustrate the deployment, servicing and recovery times.
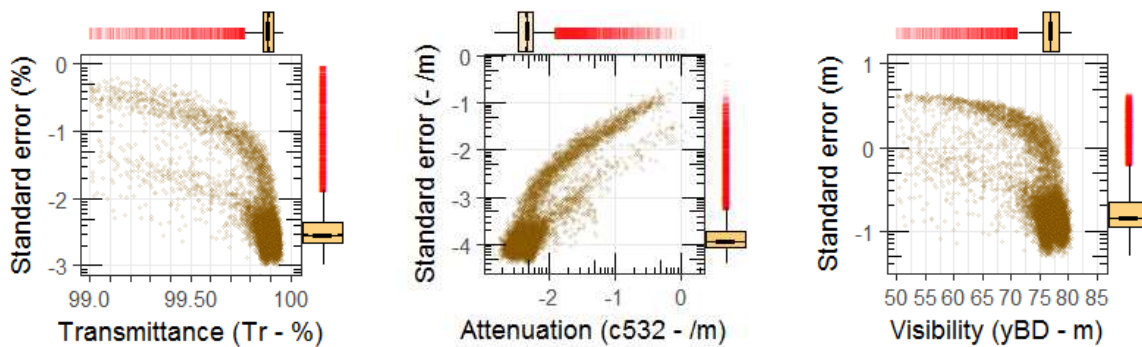
Figure 3-4: Example of standard error variances over each 60-sample burst, and distribution to water clarity measures. Details of marginal boxplots are described in Figure 3-1. Table 3-1 summarises descriptive statistics. Note: The transmittance and visibility plots are log-normal scaled, whereas attenuation is log-log scaled.

The median standard error of 60-second transmissivity (Tr) readings (0.0029%) quantifies the accuracy of the sensor to detect small temporal changes. The median standard error of beam attenuation (c532) was 0.0001 m^{-1}, equating to a standard deviation of about 0.0078 m^{-1}, is four times lower the stated manufacture precision of 0.003 m^{-1}. The median standard error in horizontal visibility (yBD) for each 60 second burst is 0.1 m over the deployment period.

The median visibility, inferred with 'reasonable' assumptions about spectral trend in attenuation, was 77.3 m (mean 76.1 ± a standard deviation of 6.5 m) over the 3-month deployment, and ranged from 3.9 to 81.3 m.

Table 3-1: **Descriptive summary statistics.** The first column (se60) of each variable is a summary on the standard error (se) of each measurement burst (60 readings). The second column (mean) is analysis summary of each measurement mean. These are illustrated as marginal boxplots in Figure 3-4 and are from 14,037 observations (of 60 burst readings). Note: Transmittance (Tr -%); Beam attenuation (c532 - /m); and Horizontal visibility (yBD – m).

| Statistic	Tr se60	Tr mean	c532 se60	c532 mean	yBD se60	yBD mean
Minimum	0.0000	74.4977	0.0000	0.0011	0.0	3.9
Maximum	3.9426	99.9720	0.6740	1.1776	4.7	81.3
1. Quartile	0.0022	99.8668	0.0001	0.0032	0.1	75.9
3. Quartile	0.0047	99.9210	0.0002	0.0053	0.2	78.6
Mean	0.0566	99.8191	0.0028	0.0074	0.4	76.1
Median	0.0029	99.8955	0.0001	0.0042	0.1	77.3
SE Mean		0.0067		0.0003		0.1
Variance		0.6348		0.0012		42.3
Stdev		0.7968		0.0347		6.5
Skewness		-18.8		19.6		-6.5
Kurtosis		408.8		448.3		52.9

3.3   Temporal variability

Temporal variability in estimates of visibility distance occurred over a range of time scales during the 3-month deployment, correlating with changes in other water quality variables at times (Figure 3-5). These include:

1. Diurnal clarity cycle (clearest around midnight and lowest around midday) associated with water temperature and dissolved oxygen.

2. Episodic decreases in clarity (day scales).
    - Small, transient decreases in clarity (< daily time steps), not associated with increased groundwater inflow (16-Oct, 17-Nov, 21-Dec, and 27-Dec).
    - Medium, short-lived (typically day) episodic decreases in clarity associated with increased groundwater inflow (03-Nov, 08-Nov, 05-Jan and 14-Jan).
    - Large and lengthy (1-2 days) clarity depression (17th January) associated with an increase in flow and increases in temperature, CDOM (fDOM) and dissolved oxygen, and a small decrease in pH and specific conductance – reflecting overland flow of surface water of contrasting water quality (significant (239.5 mm) of rainfall fell in the catchment).

3. Apparent changes in clarity over month scales, being clearest around the beginning of December (about 80 m) following the longest dry period during the deployment.
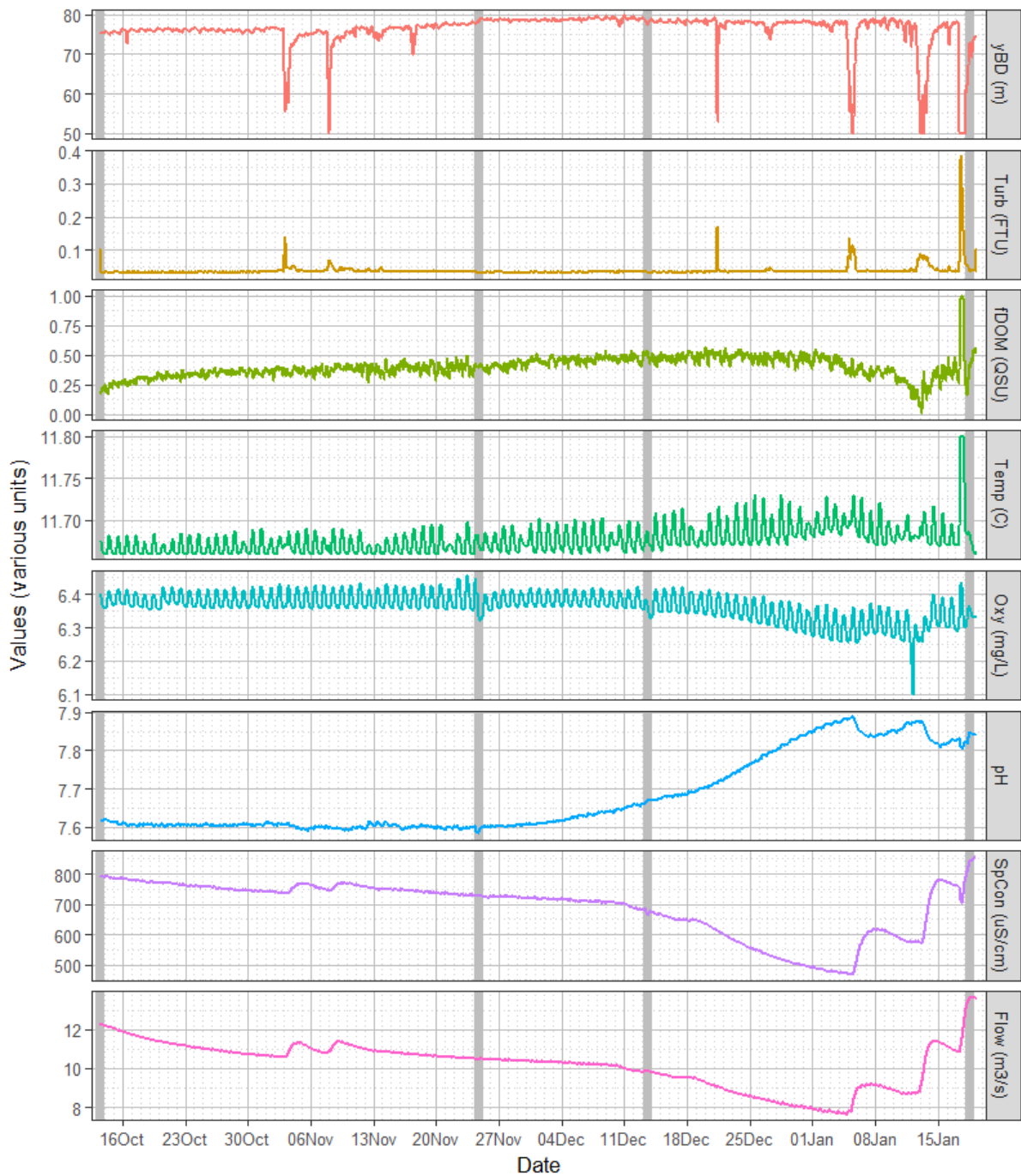
Figure 3-5: Temporal variability of visibility estimates in comparison with flow and other water quality variables continuously measured over the 3-month deployment. Note that some y-axis scales have been manually clipped to better illustrate timing of events and temporal dynamics: yBD min (4 m); Oxygen min (5.4 mg/L); Temperature max (12.7°C). Additionally, all variables except flow have a 4-hour (24 values) rolling mean applied to highlight changes and decrease noise and clutter over signal variance. Vertical grey lines denote deployment, two servicing events and recovery dates.

Flow and specific conductance were positively correlated, while flow and pH were negative correlated (Figure 3-6). The dip in dissolved oxygen concentration from late December (Figure 3-5) coincided with lower sunlight levels (data not shown). The only other feature of note is the reduction in fDOM to lowest fluorescence responses in January, occurring during more alkaline (highest pH) conditions coincident with an increase in aquifer flow that probably flushed (plant-derived) CDOM out of the springs basin.
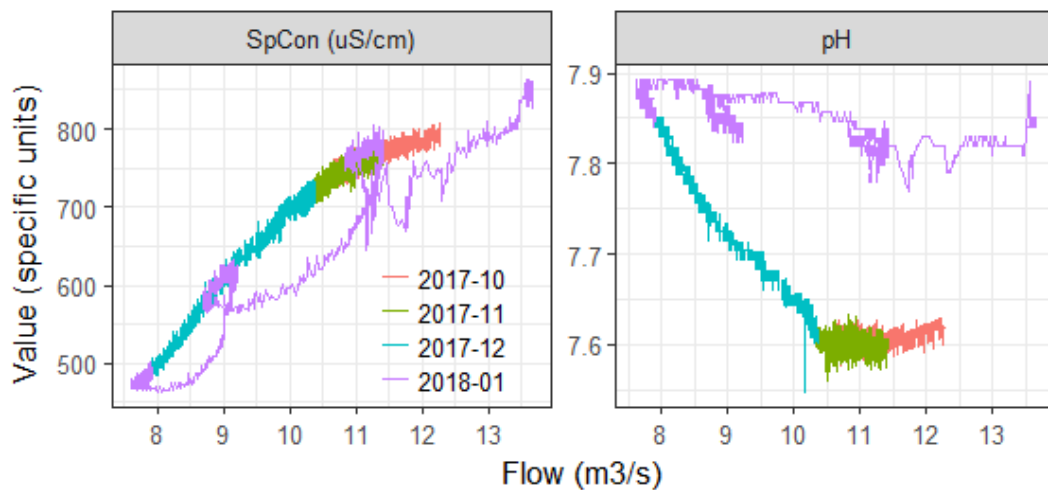
Figure 3-6: Relationships of specific conductance and pH with groundwater inflow rate. Data have been grouped by month to highlight changes in relationships.

3.3.1   Diurnal cycles

The diurnal clarity cycle had a mean range of about 2 m equivalent visibility overall, coincident with increases in light, water temperature, dissolved oxygen, and pH (Figure 3-7). Lowest visibility occurred around mid-day, while highest visibility occurred around mid-night. This diurnal pattern appears consistent with increased daytime light scattering (increased attenuation) in the springs basin due to oxygen bubbles derived from daytime photosynthesis of the abundant plant life in the springs basin. There were also clarity peaks near dawn (around 7 am) and dusk (around 10 pm), preceded and followed by decreases in clarity respectively. Small but consistent diurnal ranges in water temperature (0.03°C), specific conductance (4 µS/cm), dissolved oxygen (0.7 mg/L) and pH (0.003 units), with clarity (2 m), illustrate the sensitivity of the instrumentation and analysis for detecting and monitoring changes.
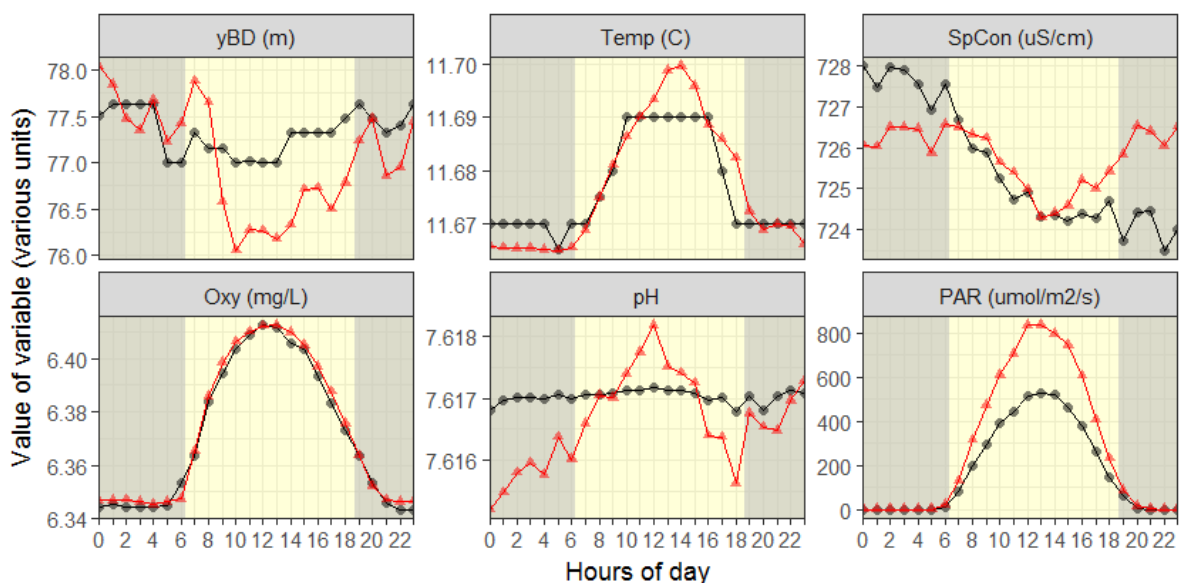
Figure 3-7: Diurnal variability of visibility estimates in comparison the other water quality variables over the 3-month deployment. Top panels, left to right, are for visual clarity, temperature, and specific conductance. Bottom panels, left to right, are for dissolved oxygen, pH and sunlight (photosynthetically available radiation; PAR). Note: Medians (grey circles) and means (red triangles) were calculated over the entire dataset, after day median normalisation of each variable to maximise diurnal signals between days with changes in variable magnitude.

3.3.2 Episodic events (day scales)

A closer inspection of three types of episodic events illustrates how decreases in apparent visibility correspond with changes in other water quality variables following catchment wide rainfall (Figure 3-8). For example, the small decrease in visibility to below 75 m on 27 December was mirrored by a small increase in turbidity (about 0.03 FTU), and lasted about 12 hours following 22 mm of rainfall in the catchment. Similarly, the decrease in visibility to below 50 m on 5 January corresponded with increased turbidity (about 0.2 FTU) and increasing flow, lasting about 12-18 hours following 34 mm of rain in the catchment. The lowest visibility was below 4 m on 17 January corresponding with the largest increases in turbidity (about 1 FTU) and increasing flow, following significant rainfall (239.5 mm within 24 hours)[1] and surface flooding. This severe weather event resulted in overland flow entering the main springs basin.

---

[1] This 24-hour rainfall corresponds with an 'Average Reoccurrence Interval' of 10 years (Brenda Clapp, TDC, pers. comm.).
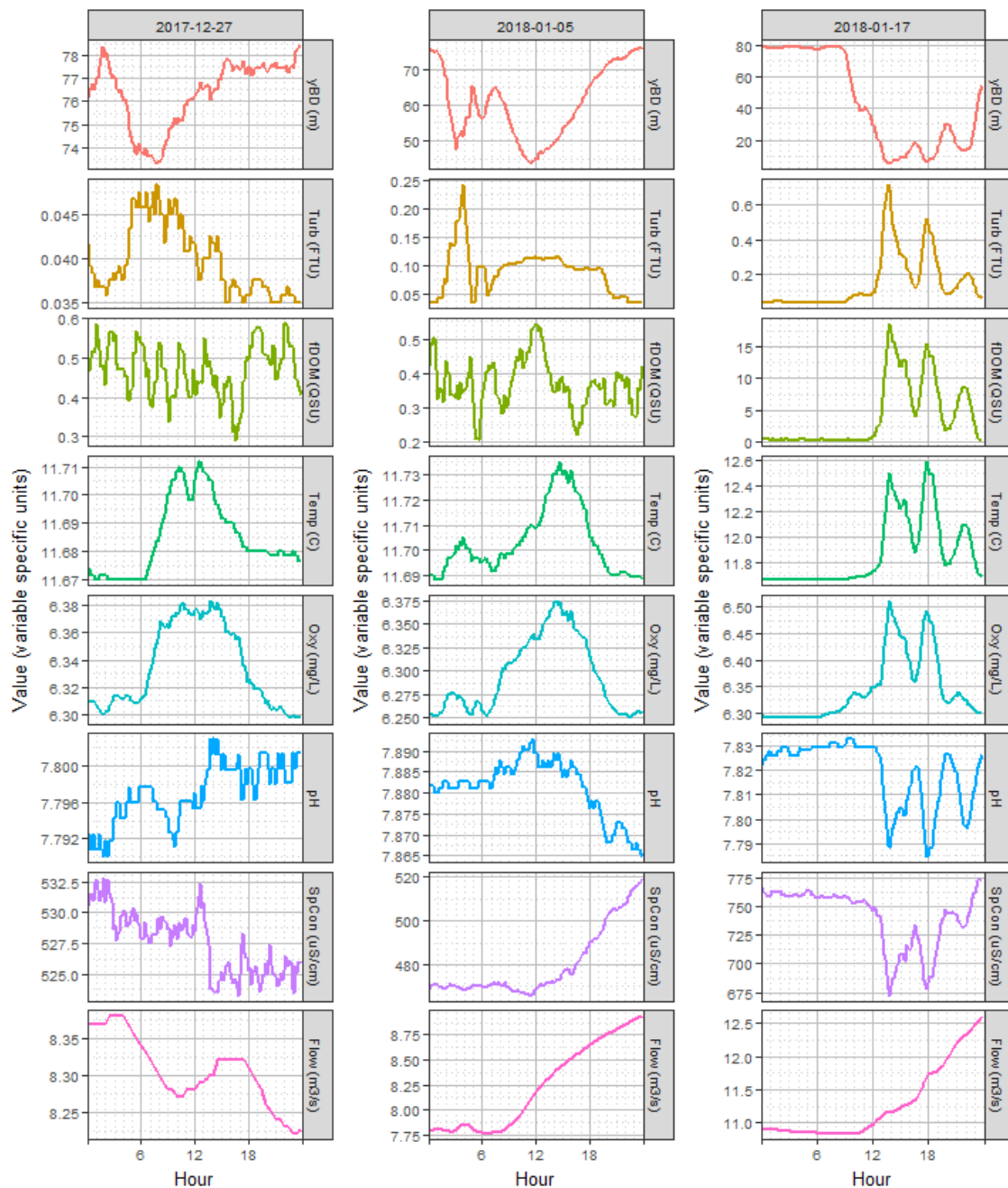
Figure 3-8: Episodic decreases in estimated visibility on three specific days in comparison with continuous measurements of other water quality variables and flow. Note: *y*-axis scales are different for each day.

3.3.3 Monthly scale observations

Over the period of transmissometer deployment, there appears to be differences in visibility over monthly scales (Figure 3-5). Because the deployment occurred from mid-October to mid-January, mid-month groups were used to ensure parity in numbers of observations. Data within each grouping failed the Shapiro-Wilks normality test so Kruskal and pairwise Wilcox tests were used to verify that medians of each group were significantly different from each other (Figure 3-9). November to December captured the clearest records in visibility (about 79 m), coinciding with the lowest rainfall, with the October to November median about 3 m less (about 76 m).
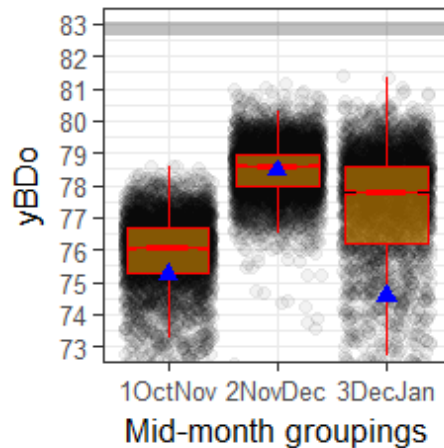
Figure 3-9: Longer term (month-scale) variation in visibility estimates. A pairwise Wilcox test verified that mid-month group median visibilities were significantly different from each other ($p < 2e^{-16}$). Note: Means (blue triangles). Visibility scale is focused around 99% of the data (whisker bounds). Details of boxplots are described in Figure 3-1.

3.3.4   Cumulative frequency distribution of visibility estimates and reduction

A cumulative frequency distribution is a useful way of illustrating the proportions (or in this case how often within the 3-month (120-day) period) a water quality variable of interest is in a specific state. Visibility estimates (Figure 3-10 A) can also be illustrated as the distance visibility has been reduced from pure water to allow a greater focus around most of the data. Figure 3-10 B indicates that visibility was reduced by more than 10 m (yBD < 73 m) only 5% of the time and was reduced by more than 33 m (yBD < 50 m) < 1% of the time. About 25% of the time the visibility was above 78 m (a 4 m reduction).
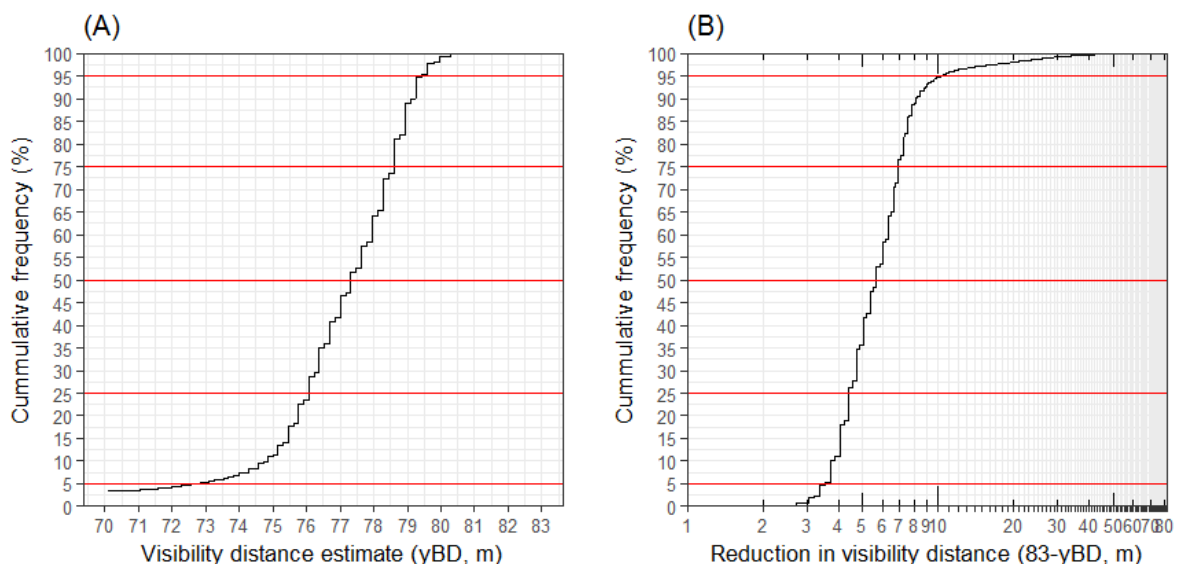
Figure 3-10: Cumulative frequency distributions of visibility reduction from pure water (A) Visibility distance estimates. (B) Reduction in visibility estimates. Note: Red lines denote the 1st and 2nd quantile, and the 5th and 95th percentile. Reduction in visibility distance has been log10 scaled to focus around most (95%) of the data.
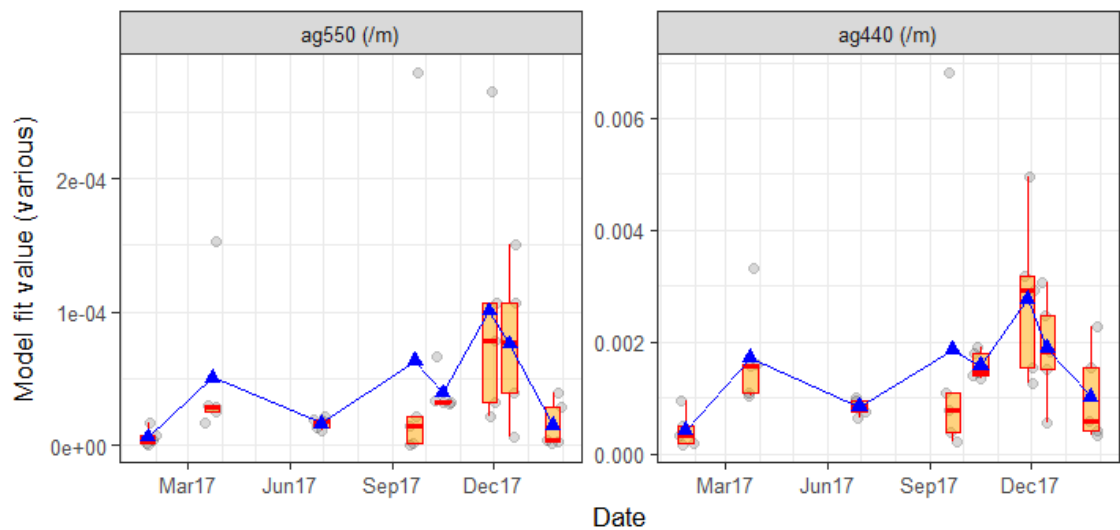

3.4   Coloured Dissolved Organic Matter (CDOM)

The measured spectra from five replicates from each sampling occasion (Appendix: Figure 7-1) were analysed by non-linear least squares (nls) spectra fit to solve for slopes, intercepts and offsets, and provide errors on their estimates (Table 3-2 and Figure 3-11). The signal to noise ratio of spectra (Appendix: Figure 7-1) was too low to extract reliable coefficients at (or around) single wavelengths of interest, except in higher UV absorbing regions of the spectra (e.g., 340 nm). Even typically reported coefficients at 440 nm have very low signals (< 0.005 m^{-1}) in these optically pure waters. The last four CDOM samples were collected during the instrumentation deployment period (Table 3-2 and Figure 3-11).

As the average estimates of ag550 (5 x10^{-5}, se = 2 x 10^{-5} m^{-1}) do not have any appreciable contribution to pure water attenuation (0.0579 m^{-1}) – less than 0.1% – CDOM absorption at 550 nm has a very small influence on horizontal visibility estimates. Although the very low absorption coefficients and relatively high variability between replicates for each monthly sampling occasion (mean CV's of 43% and 28% for ag550 and ag440, respectively) swamp differences between monthly means, there appears to be seasonal variation with higher CDOM absorption at 550 nm and 440 nm in November to December (summer), than lower absorption at other times (Figure 3-11).

Table 3-2:   **Descriptive summary statistics of CDOM absorption coefficients.** Absorption coefficient (ag) at specific wavelengths (550 nm and 440 nm) were estimated from non-linear least squares regression. Note: Five replicates were summarised on each collection.

Estimate (m^{-1})	Date (YYMM)	Mean	Standard dev	*n*	Std error	CV
ag550IE	1701	0.00001	0.00001	5	<0.00001	49
	1703	0.00005	0.00006	5	0.00003	51
	1706	0.00002	0.00000	5	0.00000	12
	1709	0.00006	0.00012	5	0.00005	85
	1710	0.00004	0.00002	5	0.00001	18
	1711	0.00010	0.00010	5	0.00004	44
	1712	0.00008	0.00006	5	0.00003	33
	1801	0.00001	0.00002	5	0.00001	53
ag440IE	1701	0.00043	0.00032	5	0.00014	34
	1703	0.00172	0.00093	5	0.00042	24
	1706	0.00085	0.00014	5	0.00006	8
	1709	0.00186	0.00279	5	0.00125	67
	1710	0.00159	0.00026	5	0.00012	7
	1711	0.00278	0.00147	5	0.00066	24
	1712	0.00189	0.00095	5	0.00043	23
	1801	0.00103	0.00084	5	0.00038	37

Figure 3-11: Coloured Dissolved Organic Matter absorption spectra model fit parameter estimates.
Boxplots of each sampling date overlain with means (blue triangles) for 550 and 440 nm wavelength coefficients (ag).

4   Discussion

Estimated median horizontal visual clarity (about 77 m) exceeds a single set of direct (black disc) measurements made in February 1993 of about 63 m (Davies-Colley and Smith 1995). Direct measures in Waikoropupū have a limited visual range (diameter of the basin is approx. 35 m), requiring a glass mirror to sight the black disc target. Ideally, a black disc target should be viewed unrestricted, with enough distance behind the target so that it is silhouetted against background water (see Davies-Colley and Smith 1995).

In keeping with the methods of the Blue Lake study, the current estimates of visual clarity were based on the latest photopic attenuation coefficients for pure water cw550 = 0.0579 m^{-1} (see Gall et al. 2013). This corresponds to a theoretical limit of about 83 m visibility, which was observed directly as black disc horizontal visibility (yBD) on one occasion in Blue Lake. The Blue Lake study supported the use of lower pure water attenuation than the value of 0.0653 m^{-1} used by Davies-Colley and Smith (1995) at the time (corresponding to 74 m visibility). This would equate to a reduction in visibility estimates from beam transmittance to about 67 m. The proportional differences of visibility estimates to pure water in both studies should be similar. Visibility estimates of Waikoropupū equate (on average) to 90% (75 m) of the theoretical maxima, and on occasions approach 98% (81 m).

The extremely high clarity of Waikoropupū is broadly comparable to that of Blue Lake (Nelson Lakes National Park) in the same region. Despite these two water bodies being unrelated geologically and hydrologically (Michaelis 1976; Gall et al. 2013), there are similarities in the dominance of spring-fed water at base flows and nearly complete particle filtration and CDOM removal during aquifer transport.

There is no direct evidence to suggest that the visual clarity of Waikoropupū has changed since early observations of Davies-Colley and Smith (1995), in consideration to methodological differences and changes in literature photopic attenuation coefficients. As ideal black disc viewing conditions are not possible in Waikoropupū, direct measures may have been underestimated and there remains uncertainty as to their accuracy. It is considered that a median of 77.3 m represents the most accurate estimate of visual clarity to date.

4.1   Methods for monitoring visibility and assessing uncertainty

The previous Envirolink small advice grant (Gall 2016) recommended continuing monitoring of the main springs with a WET Labs C-Star green beam attenuation meter after factory calibration, for at least 60 one-second stable recordings, accompanying air (maximum) and dark (minimum) benchmarks. Uncertainty remained in the field precision and accuracy of the 0.25 m pathlength to determine visibility estimates, and the best time of day to take attenuation measurements considering potential interference from microbubbles.

The application of air/dark calibrations bracketing the 3-month deployment and servicing illustrated the challenges of 'anchoring' and adjusting in-water measures with and between field calibrations (Figure 3-2). While this equated to a systematic (method) error of about 8 m (max.), a bias of about ± 5 m is realistic (this is only during the clearest times, when clarity conditions approach that for pure water). For a 50 m visibility (99 % transmittance value), the bias reduces to ± 1.5 m. The approach of using the 'highest' air statistics for the entire deployment period is conservative (lowest visibility estimates) and does not account for any potential instrumentation drift, yet provided credible transmittance values (and therefore visibility estimates) not exceeding those of pure water. WET Labs state that the C-Star transmissometer has a beam attenuation precision of 0.003 m^{-1} at 1 Hz and

recommend factory calibration about very two years, and/or when air /dark calibrations fall below specified thresholds. When considering visibility in pure water, the stated precision is about half the air calibration bias range (0.006 m^{-1}) equating to precision of about 5 m. Drift over the 3-month deployment is not known but is considered to be negligible, or at least should fall well within the field air calibration ranges measured (± 5 m). The median standard error of visibility estimates of about 0.1 m for burst sampling, and ability to discriminate diurnal variability of about ± 1 m, supports the continued use of the C-Star instrument for monitoring temporal changes in water clarity, in the absence of a commercial instrument of greater pathlength that would be more appropriate for such exceptionally clear conditions.

Monitoring of the absorption spectra of CDOM, using a 1 m pathlength liquid wavelength capillary cell, provided a sensitive assessment of the (very low) CDOM content. Absorption coefficients at ag440 (about 0.0015 m^{-1}) are 10-fold less than the previous assessment in the main springs and the Blue Lake study (about 0.011 m^{-1}, Gall et al. 2013). Although the method is sensitive enough to monitor CDOM concentration, the extremely low absorption at 550 nm (0.0005 m^{-1}) has little effect on estimates of visibility in exceptionally clear conditions. This is not surprising since water samples are pre-filtered to removed light attenuating particulates, leaving only light absorbing CDOM. This means that while CDOM provides a useful index of one component of optical purity, its blue-violet colour, it will not provide an effective method for estimating visual clarity in these extremely clear waters (i.e., it is possible for CDOM and colour hue to change (blue-violets to blues), not necessarily with any change in visual clarity).

4.2   Temporal variability in visibility estimates from beam transmittance

There was one period of about 12 hours when visibility estimates were less than 1% (4 m), and several episodic and short-lived (day scale) events when visibility fell below 60 % (50 m). However, the cumulative distribution analysis of visibility (refer Figure 3-10) confirmed that 95% of the time, visibility is above 73 m with a median of about 77 m.

The WET Labs C-Star 0.25 m pathlength green transmissometer proved sufficiently accurate and stable to track diurnal changes in visibility estimates of about 2 m (2.5%). This was coincident with an increase in dissolved oxygen of about 0.07 mg/L (1%), and an increase in water temperature of about 0.04^{o}C (0.3%). In the original study by Davies-Colley and Smith (1995), there was anecdotal evidence from the observers that measured black disc visibility was highest earlier in the morning (pers. comm.). This was speculated to be a result of micro-bubble formation during the day from photosynthesising aquatic plants. It is unlikely that such small changes in measured dissolved oxygen and water temperature would impact visibility. However, as the springs are a rapidly flushed system (see estimates of flushing times below of about 5 min), the impact of the substantial aquatic plant biomass on micro-bubble formation could have a diminished signal in the oxygen records. Although diurnal patterns in visibility are evident in the data (± 1 m), with highest visibility around midnight, other biological day time activity may also explain some of this small reduction (i.e., aquatic fish and bird foraging/movements, benthic disturbance).

Underwater images (and video) taken prior to recovery and decommissioning of instrumentation on 18 January 2018 identified a potential mechanism for some of the short-lived episodic events associated with increasing flows (seen in Figure 3-5 and Figure 3-8). 'Jets' or plumes of white sands and particles were observed percolating from the main basin vent near the deployed instruments (Figure 4-1). White sands, presumably of marble, are evident around the basin and amongst benthic vegetation, hinting at much larger disturbance periods and spatial distribution of white material. It is

likely that entrainment of white sand plumes (and/or particles from within the aquifer) associated with the release of much finer (more strongly light-attenuating) silt and clay-sized particles (say in the range 0.1-10 microns) could be the main cause of short-lived reductions in visibility.

Figure 4-1: Deployed instrumentation in Te Waikoropupū Springs. The instrument hangs suspended about 1 m off a sloping bathymetry near the springs deepest basin. Note: The 'jet' (blur) of white sands (black box), and white sands scattered around the basin area.

The two broad groups of standard error over the 60 second burst of readings (low and high) during reduced visibility suggest the presence of different types of attenuating material. Low standard errors over 60 readings indicates uniformity (less noise) during readings as opposed to high standard errors indicating less uniformity (high noise) during readings (larger particles, less abundant). This is illustrated in Figure 4-1, where smaller particles tend to produce a uniform background haziness (cloudiness or milky appearance, where individual particles cannot be seen), and larger particles that can be seen suspended in the water (mobile sands and detritus). There is obviously a combination of particle size and type effects at different times and therefore a range of standard errors in each 60 second burst of readings.

The lowest visibility estimates (< 10 m) occurred with overland flows entering the springs associated with a severe weather event on 17 January (239.5 mm of rainfall). Not unexpectedly this event was accompanied by increases in water temperature (12.7°C) above the springs typically stable 11.6-11.7°C range (Young et al. 2017), with an increase in fDOM, and the author's observation of recent flooding impacts on the surrounding land. Using these water quality variables as tracers, the introduced higher temperature and turbid water was flushed by main spring flow exchange in about 12 hours. Michaelis (1976) estimated a mean holding time (flushing time) of the Main Spring of about 4.4 minutes, based on its volume (2200 m³) and discharge rate of 9.6 m³/s. When considering the flushing of introduced material in an idealised system, the initial concentration follows an exponential decline (Monsen et al. 2002), taking about 5 flushing times (e^{-5}) for a dilution to 1% of the initial concentration. Therefore, under idealised conditions of complete basin mixing, any introduced suspended material should be flushed to 1% of initial concentrations in about 30 minutes.

This monitoring documents episodic events on day scales and recovery over about 12 hours – probably reflecting inflow of turbid water at the well-vegetated margins of the spring basin which are much less rapidly flushed than the central basin. While periodic declines in visual water clarity occur in Waikoropupū, these are generally short-lived and are to be expected in a high rainfall location like Golden Bay (i.e., at times, flood waters from the surrounding land will enter the spring and impact on water quality). For most of the time (95%), water clarity was greater than 73 m.

A longer deployment, ideally over an annual or multi-year cycle, would be required to assess seasonal patterns in the clarity regime with any confidence. The bi-monthly and monthly laboratory CDOM absorbance records and analysis hint at seasonality, consistent with the expected seasonal cycle of plant growth. The month-scale variation in visibility estimates (Figure 3-9) also hints at longer term variability.

The TDC's historical records of aquifer flow and rainfall help provide both seasonal and inter-annual context for the 3-month continuous monitoring deployment period (Figure 4-2). Clearly, there are seasonal patterns, with higher aquifer flows and rainfall during winter seasons, followed by lower flows and rainfall during late-summer-autumn seasons.[2] Late summer-autumn 2017 appears to be an unusual year, with higher flows and more rain than previous years (i.e., less pronounced dips). As shown in visibility estimates in comparison to flow, increasing flows (accelerating currents) are associated with reduced visibility, and therefore historical and future records of changes in the magnitude, prevalence and timing may modify visibility. Conversely, the magnitude and prevalence of low flow periods may indicate the highest visibility periods. Surface flooding of Waikoropupū, as occurred around 16-18 January 2018 (impacting on visibility), will also have occurred at other times in other years where high persistent rainfall periods coincided with high flow rates (Figure 4-2). What is evident from the decadal patterns is that although there are some seasonal trends, there are also inter-annual differences between the magnitude and timing of flow and rainfall events, and therefore by inference natural variations in visibility.
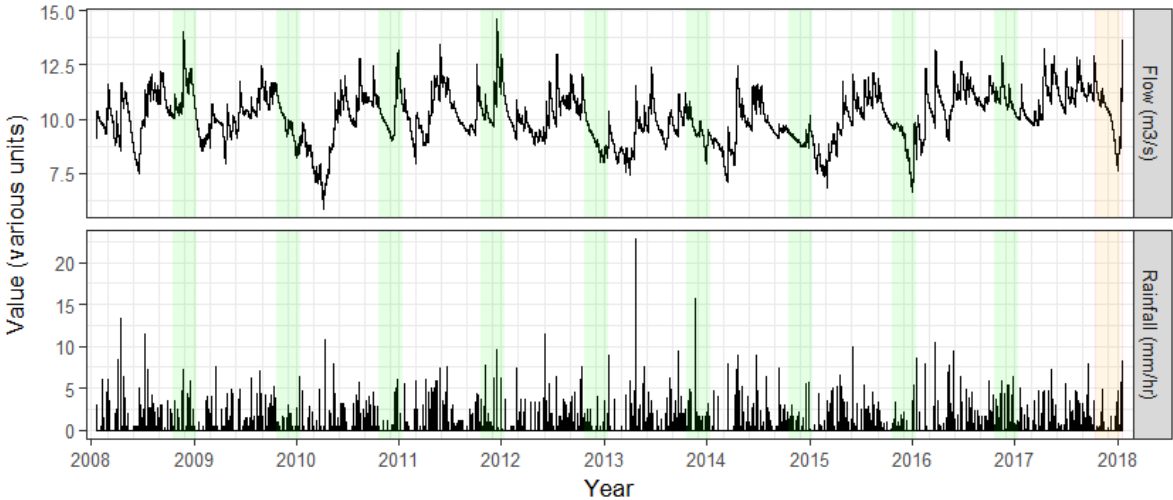
Figure 4-2: Decadal historical records of flow and rainfall Context of flow regime and rainfall during deployment (orange) with other periods in previous years (green).

---

[2] Outputs from the Cobb power dam will also influence flow variability in lower rainfall periods (Rob Smith, TDC, pers. comm.).

5 Conclusions

The three-month deployment of a green beam transmissometer in Te Waikoropupū Springs, between October 2017 and January 2018, has partially characterised the 'clarity regime' of this water body. A median visual clarity of about 77 m (mean 76 ± 7 m standard deviation) was estimated with 'reasonable' (but inevitably uncertain) assumptions about sensor air calibrations and the spectral trend of light attenuation. About 95% of the time visibility was above about 73 m, confirming the extremely high clarity of Waikoropupū and, on occasion, the inferred visibility (maximum about 81 m) approached that of pure water (about 83 m). Overall, the visual clarity of Waikoropupū is similar to that reported by Gall et al. (2013) for Blue Lake. Furthermore, there is no direct evidence from this study to indicate that there has been any significant change in visual clarity in Waikoropupū in the 25 years since the direct measurement of 63 m made by Davies-Colley and Smith (1993).

The small diurnal cycle of clarity (± 1 m) with highest visibility at midnight, and lowest around mid-day, is plausibly related to the diurnal cycle of photosynthesis in the springs basin of plants that release (light-scattering) oxygen bubbles during the day. Some short-term (hours to days) episodes of lower clarity coincide with increasing flow (accelerating currents) which entrains white marble sands and, possibly, finer (more strongly light-attenuating) particulates. Several short-lived (about 12-hour) episodes of surface flooding were captured during the deployment with a notable one occurring in mid-January where turbid water entered the main springs basin and resulted in the lowest observed clarity (4 m). Overall, the fluctuations observed in visual clarity over the deployment period can be attributed to natural variation in rainfall and flow.

The deployment confirmed that, while it is operating beyond normal limits, a 0.25 m pathlength WET Labs C-Star green beam transmissometer is – with careful calibration – precise and accurate enough to estimate visual clarity and monitor temporal changes in extremely clear, optically pure spring waters. Further, coupling a transmissometer deployment with continuous monitoring of key related water quality variables (temperature, dissolved oxygen and specific conductivity) can help explain observed short-term temporal dynamics in visual clarity and episodic low-water-clarity events.

Measurements of CDOM served to emphasise the extreme optical purity of water from Waikoropupū. The mean CDOM absorbance at 440 nm was 0.00152 m^{-1} and is consistent with the blue-violet colour of pure water. However, the contribution of CDOM to reduced visual clarity was negligible so CDOM cannot serve as an index of visual clarity.

5.1 Recommendations

1. Implement a water clarity monitoring programme at Waikoropupū that includes visual clarity and CDOM. The former could be based on a short-term annual or multi-year (e.g., 5-yearly) campaign-based deployment, similar to that outlined in this report using a WET Labs C-Star 0.25 m pathlength green beam transmissometer (or equivalent). Alternatively, consider the collection of in-*situ* discrete (dip-mode) beam transmissometer measurements alongside existing 'seasonal' (3-month) State of the Environment groundwater quality sampling, or monthly surface water quality sampling. If the latter approach is adopted, it must be emphasised that making accurate measurements will be challenging, and will require great care to avoid disturbance of plants or sands that might suspend fine particles. The timing and duration of any monitoring will need to consider the types of small scale and seasonal variability in visual clarity illustrated in this report.

2. For any discrete (dip-mode) measures using a WET Labs C-Star (or equivalent):

- Strictly adhere to the field cleaning and calibration protocols outlined on the WET Labs website, with raw value recordings taken for at least 60 readings at 1 second intervals. Air and blank calibrations should be done (with great care) under laboratory controlled conditions whenever possible.

- Obtain field measurements at the same time of day on each sampling occasion, ideally as early in the day as practical and before oxygen bubbles are produced from photosynthesising aquatic plant life.

- Deploy the instrument in the water, as opposed to removing a water sample for measurement, and leave in position for as long as practical, but for a minimum of 60 'stable' readings at 1 second intervals.

- Graphically track raw instrument response to verify stability and avoid measurement collection during stabilisation drift and/or microbubble formation on optical surfaces.

- Calculate statistics to allow γBD to be estimated with the required precision and estimate errors.

- Establish and maintain an instrument-specific inventory of calibration checks, with assessment of which calibrations to apply over multiple attempts or sampling periods. This is necessary to avoid compromising *in situ* measurements with inaccurate calibrations.

3. For CDOM, continue to collect water samples in at least triplicate from the main spring, on at least a quarterly basis, for long pathlength absorption analysis in a laboratory, to track changes in colour, a key aspect of the optical purity of Waikoropupū.

6   Acknowledgements

References

Bricaud, A., Morel, A., Prieur, L. (1981) Absorption by Dissolved Organic Matter of the Sea (Yellow Substance) in the Uv and Visible Domains. *Limnology and Oceanography*, 26(1): 43-53.

Chambers, J., Cleveland, W., Kleiner, B., Tukey, P.A. (1983) Comparing Data Distributions. *Graphical Methods for Data Analysis (Bell Laboratories)*: 47-73.

Davies-Colley, R. (1988) Measuring Water Clarity with a Black Disk. *Limnology and Oceanography*, 33(4): 616-623.

Davies-Colley, R. (1992) Yellow Substance in Coastal and Marine Waters Round the South Island, New Zealand. *New Zealand Journal of Marine and Freshwater Research*, 26: 311-322.

Davies-Colley, R., Smith, D. (1995) Optically Pure Waters in Waikoropupu ('Pupu') Springs, Nelson, New Zealand. *New Zealand Journal of Marine and Freshwater Research*, 29(2): 251-256.

Duntley, S.Q. (1963) Light in the Sea. *Journal of the Optical Society of America*, 53(2): 214-233.

Gall, M. (2016) Water Clarity Monitoring. Te Waikoropupu Springs. *NIWA Client Report*, 2016101WN: 18.

Gall, M., Davies-Colley, R., Merrilees, R. (2013) Exceptional Visual Clarity and Optical Purity in a Sub-Alpine Lake. *Limnology and oceanography*, 58(2): 443-451.

Michaelis, F.B. (1976) Physico-Chemical Features of Pupu Springs. *New Zealand Journal of Marine and Freshwater Research*, 10(4): 613-628.

Monsen, N.E., Cloern, J.E., Lucas, L.V., Monismith, S.G. (2002) A Comment on the Use of Flushing Time, Residence Time, and Age as Transport Time Scales. *Limnology and oceanography*, 47(5): 1545-1553.

SBE. (2011) *Calculating Calibration Coefficients for Wet Labs C-Star Tranmsissometer*. Application Note No. 91. ftp://misclab.umeoce.maine.edu/users/optics/classFTP/Portfolio/Hyperlink/Cstar_seabird_calibration.pdf

Team, R.D.C. (2017) R: A Language and Environment for Statistical Computing. *R Foundation for Statistical Computing Vienna Austria*. http://www.R-project.org

Young, R., Fenwick, G., Fenemor, A., Moreau, M., J., T., McBride, G., Stark, J., Hickey, C., Newton, M. (2017) *Ecosystem Health of Te Waikoropupū*. Prepared to Support Decision Making by the Takaka Freshwater Land Advisory Group. , 2949: 47.

Zaneveld, J., Pegau, W. (2003) Robust Underwater Visibility Parameter. *Optics Express*, 11(23): 2997-3009.

7 Appendix

7.1 Additional plots
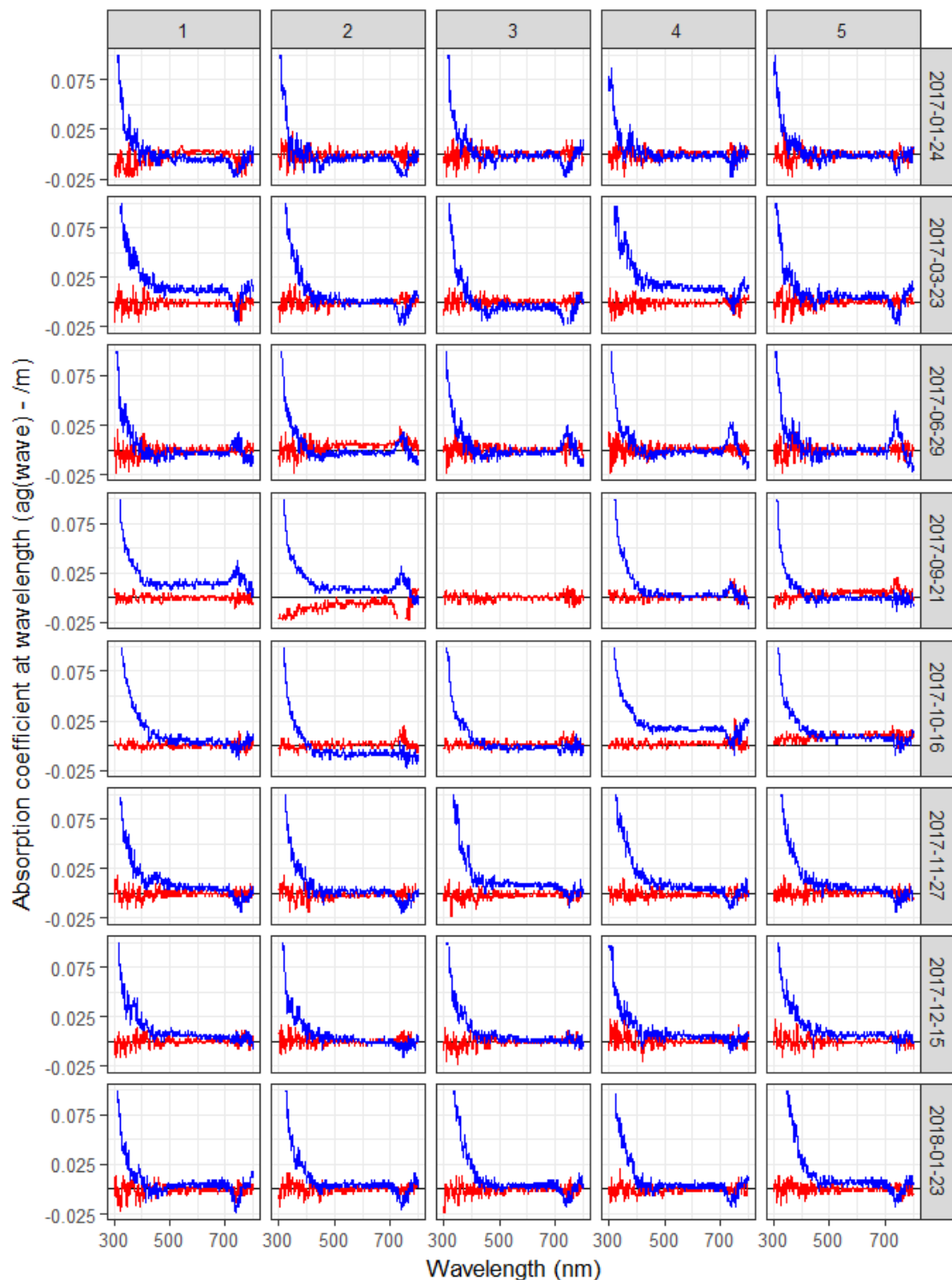
Figure 7-1: Coloured Dissolved Organic Matter absorption spectra (ag – m⁻¹). Replicate spectra (blue) and their nanopore water blanks (red) from each collection. Data are summarised in section 3.4 and Figure 3-11.

7.2   WET Labs-C-Star transmissometer protocol

Wetlab supplies several documents which outline the calculations, procedures for use and functional checks and cleaning methodologies on their website (http://WET Labs.com/C-Star). Users of this instrument should be familiar with these documents and follow recommended protocols. This is especially important when the water is very clear and the instrument is operating close to its limit of sensitivity. In particular, should the transmissometer fall outside these functional checks after careful cleaning, it should be returned to the factory for diagnostics and re-calibration. WET Labs recommends annual factory servicing, particularly to check seals and ensure there is no moisture inside the instrument housing which causes condensation behind optical lenses. If this is not apparent, the instrument should be factory calibrated every two years (its warranty period).

There are a number of recommendations to ensure high precision (low variability around reading) and accuracy (high confidence in value of readings) using the C-Star with its supplied WETView software:

1.   Adjust the settings of instrument to output data at 1 second intervals.

2.   Collect at least 60 seconds worth of 'good' data for each measurement (air, blocked, sample). This can be done within the same file (noting time ranges for each measurement) or as separate files, naming appropriately. An air and dark sample should only be needed at the beginning of day's sampling. We suggest using a reverse date file naming (e.g. YYYYMMDD_Type.raw: For example, 20161005_Air.raw). This ensures files will sort in order of date.

3.   Measure with the instrument directly in the water (in-situ), ensuring optical surfaces are free of air and bubbles. Visualise the data trace using the plot tab on WETview and once stable, record a raw file for at least 60 samples. This should minimise any contamination and provide a stable reading. If the instrument track is not stable over the 60 seconds, inspect the instrument, clean the optical surfaces and repeat the measurement procedure.

4.   If an *in-situ* measurement is not possible, collect a sample using a 'very clean' container (rinse several times with sample water) and dispense into a black pipe with endcap just larger than C-Star – or use the black pipe to fill with sample. Place C-Star in the pipe and move up and down to assist in mixing. Note if the data trace is stable and record a raw file for at least 60 samples. If the trace decreases or increases over this period, bubbles are forming on the optical faces or particles are settling out. Repeat until the most stable trace possible is recorded. Take readings as soon as practical and before water warms to air temperature as this will cause degassing of water.

5.   Import the saved raw files into EXCEL. Undertake quality control and calculate statistics (e.g. mean, median, standard deviation; standard error, etc.). Use these values for further calculations.

Recording at least 60 samples ensures statistical robustness and enables diagnostics to be compared against published noise and expected deviations of air and dark calibrations over time. It also ensures confidence in an accurate representation of the sampling and if measurements are being affected by drift over the sampling period. It should provide a true statistic of natural variability of the calibrations and sampling.